

Pressure-induced metal-insulator transition and absence of magnetic order in FeGa₃ from a first-principles study

J. M. Osorio-Guillén*

Instituto de Física, Universidad de Antioquia, Medellín, Colombia and Centro de Ciências Naturais e Humanas, Universidade Federal do ABC, Santo André, SP, Brazil

Y. D. Larrauri-Pizarro and G. M. Dalpian

Centro de Ciências Naturais e Humanas, Universidade Federal do ABC, Santo André, SP, Brazil

(Received 13 September 2012; published 3 December 2012)

The intermetallic compound FeGa₃ is a narrow-gap semiconductor with a measured gap between 0.2 and 0.6 eV. The presence of iron *d* states on the top of the valence band and on the bottom of the conduction band, together with its moderate electronic correlation ($U/W \sim 0.6$), have led to the question of whether there is magnetic order in this compound. We have examined the possible presence of magnetism in FeGa₃ as well as its electronic structure at high pressures, using the density functional theory (DFT) + U method with the intermediated double-counting scheme. We have found that for an optimized value of the Yukawa screening length λ , there is no magnetic moment on the iron ions ($\mu = 0$), implying that FeGa₃ is nonmagnetic. We have also found that around a pressure of 25 GPa a metal-insulator transition takes place.

DOI: [10.1103/PhysRevB.86.235202](https://doi.org/10.1103/PhysRevB.86.235202)

PACS number(s): 71.20.Nr, 71.30.+h, 31.15.V–

I. INTRODUCTION

Intermetallic narrow-gap semiconductors have very interesting electronic, magnetic, thermoelectric, and transport properties.^{1–15} Among these compounds, FeGa₃ (which has the Fe *d* states on the top and the bottom of the valence and conduction bands, respectively) has emerged as an attractive compound to study the regime between weakly and strongly correlated materials.^{5–8,11–15} On one hand, some experimental measurements of the conductivity, magnetic susceptibility, Mössbauer spectra, specific heat, etc., have not shown distinctive features of a very strong electronic correlation, and these results also indicate the absence of magnetism in this compound.^{10,11} Nevertheless, the size of the ratio between the on-site Coulomb interaction (characterized by the Hubbard U parameter) and the bandwidth of the Fe *d* electrons ($U/W \sim 0.6$) is comparable to other correlated materials.^{5,8,14,16,17} These clues have led to a first-principles density functional theory (DFT) + U study of the magnetic order in this compound, showing evidence of a “spin-singlet” coupled Fe dimer with antiferromagnetic (SS-AF) order (with a magnetic moment of $0.63\mu_B$ /Fe ion for Hubbard $U = 2$ eV). These results were obtained using the fully localized atomic limit (FLL) for the double-counting (DC) term for DFT + U .⁸ A recent muon spin rotation measurement suggests that the existence of a spin polaron band is consistent with the SS-AF scenario, in which Fe moments exist at all temperatures.³ However, due to the moderate electronic correlation in this material, the FLL is not appropriate to study this compound, and it could lead to an erroneous magnetic ordered solution.^{16,18} It is pertinent to reexamine the possible presence of magnetic order in this compound using DFT + U with a suitable DC scheme for systems presenting weak to moderate electronic correlation, such as the intermediate double counting (INT DC).^{17,18}

On the other hand, it is known that low-electron doping tremendously modifies the electronic and magnetic properties of FeGa₃.^{6,7} Remarkably, electron doping of this compound

induces a crossover to metallic behavior and shows some physical properties that resemble strongly correlated metals. Also, Co doping creates local magnetic moments, presumably on Co ions, but there is not a conclusive explanation of the mechanism that triggers the occurrence of magnetic order in this compound.⁷ The effect of external pressure provides a very useful means to modify the strength of the hybridization between the Fe *d* and Ga *s* and *p* states, making it possible to study systematically the electronic and magnetic structure without introducing any chemical perturbation, charge carriers, or defects. While some chemical substitution studies of FeGa₃ have revealed a metal-insulator transition (MIT) due to electron doping,^{6,7} the effect of volume compression has not been employed yet. In this work we show that in FeGa₃ there is no presence of SS-AF and propose that the application of an external pressure on this compound changes its electronic structure profoundly, causing a MIT around 25 GPa.

II. METHOD OF CALCULATION

Spin-polarized first-principles DFT and DFT + U calculations have been carried out using the full-potential augmented-plane-wave method with local orbitals (FP-APW + lo) as implemented in the ELK code.¹⁹ For the exchange-correlation energy functional we have employed the generalized gradient approximation (GGA).²⁰ The DFT + U approach is applied following the methodology described in Ref. 18 with Yukawa screening^{16,18,21} and the INT-DC scheme.^{17,18} In this DFT + U implementation one adds a Hartree-Fock correction to the DFT-GGA Hamiltonian, where the kernel of the interaction term is the bare Coulomb interaction ($1/r_{12}$). One can choose an atomic basis function to evaluate the interaction term, allowing us to write down the radial part of the Coulomb interaction by the bare Slater integrals $F^{(k)}$. These $F^{(k)}$ are mostly affected by screening effects, and one should replace them by the screened Slater integrals $F_I^{(k)}$, which are the parameters of the DFT + U scheme. These $F_I^{(k)}$ can be obtained

by using a Yukawa interaction ($e^{-\lambda r_{12}}/r_{12}$) instead of the bare Coulomb interaction, where we introduce the Yukawa screening length λ to scale the screening effects. This approach has the advantage that it determines the ratio between the different $F_i^{(k)}$ in a more realistic way (instead of the $U = F_i^{(0)}$ and $J = \frac{F_i^{(2)} + F_i^{(4)}}{14}$ parameters individually in the case of d orbitals), and it is only necessary to find one parameter, i.e., λ .

The muffin-tin (MT) radii of Fe and Ga are set to $R_{\text{MT}}^{\text{Fe}} = 2.00$ a.u. and $R_{\text{MT}}^{\text{Ga}} = 1.45$ a.u., respectively. The parameter $R_{\text{MT}}^{\text{Fe}}|\mathbf{G} + \mathbf{k}|_{\text{max}}$ governing the number of plane waves in the FP-APW+lo method is chosen to be 9.5. The Brillouin zone (BZ) is sampled with a uniformly spaced \mathbf{k} grid of $6 \times 6 \times 6$ for the structural relaxation and $16 \times 16 \times 16$ for the calculation of the dispersion relation $E(\mathbf{k})$ and the total and site-projected densities of states (DOS).

III. RESULTS AND DISCUSSION

FeGa₃ has a simple tetragonal crystal structure, which belongs to the nonsymmorphic space group $P4_2/mnm$, with 16 atoms in the unit cell.^{14,15} Fe ions are located at Wyckoff position $4f$ ($u, u, 0$), point group C_{2v} ; one type of gallium, Ga₁, is located at Wyckoff position $4c$ ($0, \frac{1}{2}, 0$), point group C_{2h} , and the other type of gallium, Ga₂, is located at Wyckoff position $8j$ (u, u, w), point group C_s . One of the main characteristics of this crystal structure is the presence of two Fe dimers: the first dimer is placed along the (110) direction on the plane $z = 0$, and the second dimer is placed along the (1 $\bar{1}$ 0) direction on the plane $z = \frac{1}{2}$. Due to the relative isolation of each dimer from one another, the SS-AF ordering was proposed.⁸ In the following sections the choice of double-counting scheme in the DFT + U method and the effects of external pressure on the electronic and magnetic structure of FeGa₃ are presented.

A. Double-counting scheme

In DFT + U there are two usual choices for the DC scheme that are adopted depending on the electronic correlation limit to which the material is closer. On one hand, for weakly correlated metals, the *around mean field* (AMF) limit²² creates an artificial atomic polarization around the uniform occupations produced by local and semilocal exchange-correlation functionals [e.g., local-density approximation (LDA) and GGA], and it always gives a negative correction to the total energy. On the other hand, for strongly correlated systems, such as antiferromagnetic Mott insulators, one considers an isolated atom in contact with a reservoir of electrons. In this DC scheme, which is called the *fully localized atomic limit*,^{23,24} the LDA (GGA) levels are shifted depending on their occupations; fully empty states are moved upward by $(U - J)/2$, and fully occupied states are rigidly shifted downward by $(U - J)/2$. In addition, the FLL always gives a positive correction to the total energy. However, for real systems and especially in moderately correlated materials, the occupation numbers lie somewhere between the above two limits. For these cases it is more appropriate to apply the *intermediate double-counting* scheme,¹⁷ which is a linear interpolation between the two limits corresponding to AMF and FLL. Moreover, the INT DC has the correct formula (in the

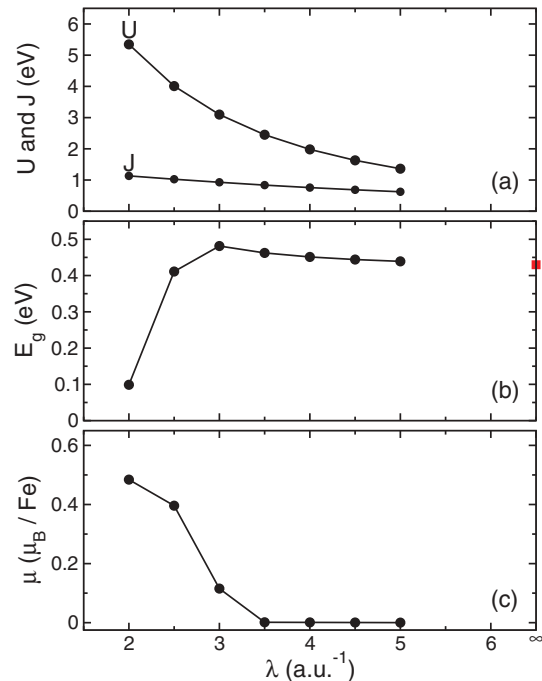


FIG. 1. (Color online) (a) Calculated Hubbard parameter U and intra-atomic exchange parameter J , (b) band gap E_g and (c) magnetic moment per Fe ion μ as a function of the Yukawa screening length λ . The red square is the calculated band gap by means of GGA.

DFT sense) for the total energy since it gives zero correction to it. Other crucial aspects for us to choose the INT DC is that one can, in principle, treat on an equal footing more itinerant and more localized systems, and it turns out that the use of the INT DC is very critical to obtaining the correct magnetic structure of several compounds.^{16,18} Additionally, by using the Yukawa screening methodology for the Slater parameters, we need to find only one free parameter, i.e., the Yukawa screening length λ or, if preferable, the Hubbard U parameter appropriate to the physical system instead of the two usual parameters for d orbitals: U and J .^{18,21}

Figures 1(a)–1(c) show the variation of the Hubbard U and intra-atomic exchange parameter J , the calculated band gap E_g , and the magnetic moment per Fe ion μ as a function of λ for the experimental crystallographic parameters¹⁴ of FeGa₃ and choosing the SS-AF spin configuration described in Ref. 8. When the value of λ is decreased, we can observe in Fig. 1(a) that the calculated U ranges from small to moderate (1.4–5.3 eV), whereas J goes from 0.6 to 1.1 eV. The dependence of the calculated E_g follows the expected trend to increase its value compared to the GGA band gap [red square in Fig. 1(b)] when going from small to moderate values of U ; this happens until it reaches its maximum value for $U = 3.1$ and $J = 0.93$ eV ($\lambda = 3$ a.u.⁻¹). For larger values of U the band gap starts to decrease abruptly. This could be due partly to the overshooting of U , which causes an excess of the hybridization of Fe d and Ga p states in the valence band, and to the big exchange J . Finally, we have found that for small to moderate values of U there is no magnetic moment in the Fe ions. Nevertheless, for $U = 3$ eV and larger values the localization of Fe d electrons becomes stronger and, together with the huge J , yields a small magnetic moment on the Fe

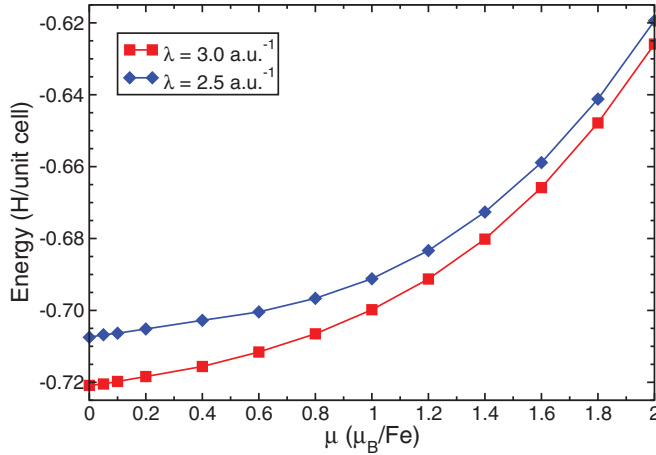


FIG. 2. (Color online) Calculated total energy per unit cell as a function of the magnetic moment per Fe ion. Red squares and blue diamonds are the obtained values for $\lambda = 3.0$ and 2.5 a.u. $^{-1}$, respectively.

ions with the SS-AF ordering. However, the occurrence of this magnetic order will be ruled out in the next section. With these findings, we have selected $\lambda = 3$ and $\lambda = 2.5$ a.u. $^{-1}$ ($U = 3.1$, $J = 0.93$ eV and $U = 4.0$, $J = 1.0$ eV, respectively) to carry out the remainder of this work because they give a good estimate of E_g and the possibility of SS-AF ordering.

B. Magnetic structure and the equation of state

In a previous study of the electronic and magnetic structure of FeGa₃, a SS-AF ordering with a magnetic moment of $0.63\mu_B/\text{Fe}$ ion for $U = 2$ eV and $J = 0.625$ eV was found.⁸ However, an exhaustive search for the validity of the SS-AF solution was not carried out. Also, the effects of crystallographic relaxation on the magnetic structure were not investigated for this compound. We have performed both types of calculations in order to elucidate the validity of the SS-AF ordering.

To investigate the stability of the SS-AF solution, we have calculated the total energy per unit cell as a function of the magnetic moment per Fe ion using the constrained fix-spin moment energy functional and the Yukawa screening lengths of 3.0 and 2.5 a.u. $^{-1}$ (note that for $\lambda \rightarrow \infty$, i.e., GGA, there is no magnetic moment in the Fe ions). We have done these calculations for the experimental crystallographic parameters to be consistent with previous work.⁸ Figure 2 shows that the obtained values of $\mu = 0.12$ and $0.40\mu_B/\text{Fe}$ for $\lambda = 3$ and 2.5 a.u. $^{-1}$ are not stable solutions. In fact, the global minimum for both Yukawa screening lengths is located at $\mu = 0$. This rules out the existence of the SS-AF ordering and corroborates the experimental magnetic studies about this compound, where magnetism was not found.^{7,10,11,14}

To further investigate this issue, we have also studied the effects of external pressure on FeGa₃. Figures 3(a)–3(d) show the total energy of the unit cell, the external pressure, the interionic distances, and magnetic moment per Fe ion in terms of the reduced volume ($\frac{\Omega}{\Omega_0}$). In Fig. 3(a) it is observed that the GGA nonmagnetic solution is more stable for the equilibrium volume, where the calculated stabilization energies ($\Delta E = E_{\lambda \rightarrow \infty} - E_\lambda$) are -8.6 and -76.16 meV/Fe for

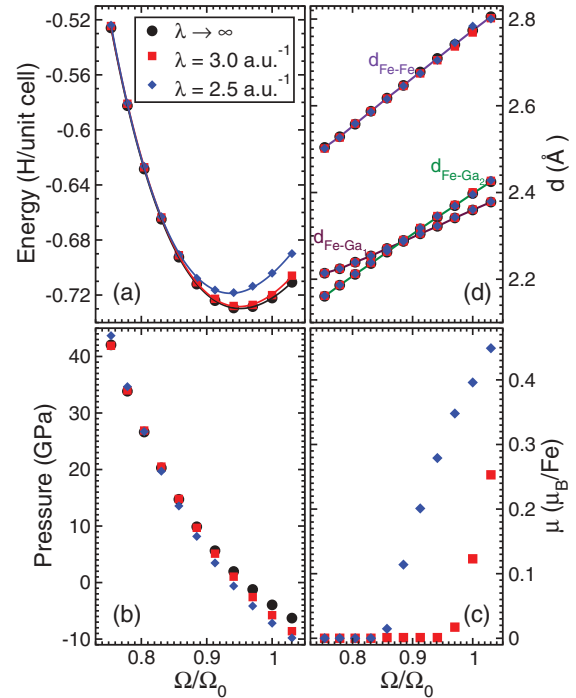


FIG. 3. (Color online) Calculated equations of state (a) $E(\frac{\Omega}{\Omega_0})$ and (b) $P(\frac{\Omega}{\Omega_0})$, (c) magnetic moment per Fe ion, and (d) interionic distances for the Yukawa screening lengths $\lambda = 3, 2.5$ and $\lambda \rightarrow \infty$ (GGA). Ω_0 is the experimental volume (Ref. 14).

$\lambda = 3$ and 2.5 a.u. $^{-1}$, respectively. These results are a further corroboration of the absence of magnetic order in FeGa₃. The calculated equilibrium volume and bulk modulus are shown in Table I. These volumes are in much better agreement with the experimental volumes than the ones calculated by means of LDA.¹⁴ It is noteworthy to observe that the calculated GGA equation of state (EOS) is lower for all the calculated reduced volumes from 1.01 to 0.85 compared to the DFT + U calculated EOS. Moreover, for reduced volumes smaller than 0.85 the GGA and DFT + U calculated EOS converge to the same total energy values. For $\lambda = 2.5$, this happens when the calculated Fe magnetic moment collapses [Fig. 3(c)]. At the pressure range between 15 and 42 GPa the electronic correlation becomes weak, and the semilocal exchange-correlation functional is sufficient to describe the physics of this compound. Additionally, we can observe in Fig. 3(d) the

TABLE I. Calculated parameters of the equation of state of FeGa₃ for different values of the Yukawa screening length λ . To fit our calculated energies we have used the methodology described in Refs. 25 and 26, finding that the best fits are given by a polynomial Eulerian strain Birch-Murnaghan EOS of fifth order. The experimental volume is given in parentheses.

λ (a.u. $^{-1}$)	Ω (\AA^3)	B (GPa)
∞	244.78	113.45
3	244.81	120.67
2.5	240.25 (257.09) ^a	127.20

^aRef. 14.

variation of the interionic distances. The Fe-Fe dimer distance decreases with the applied pressure to values close to the Fe bcc structure (2.4825 Å). More significant, it is the change in the distances between Fe-Ga₁ and Fe-Ga₂, where it is observed that both interionic distances decrease with pressure, and it is remarkable that around $\Omega/\Omega_0 \approx 0.85$, the Fe-Ga₁ distance (both ions are on the same plane) becomes larger than the Fe-Ga₂ distance. These have a profound effect on the hybridization of the Fe *d* and Ga *s* and *p* states and the character of the top valence bands, as discussed in the next section.

C. Electronic structure

The effect of external pressure on the electronic structure is an important probe to modify the strength of the hybridization between the Fe *d* and Ga *s* and *p* states. This allows the possibility to study systematically the electronic structure without introducing any chemical perturbation, charge carriers, and defects. Figures 4(a)–4(c) and 5(a)–5(c) show the calculated dispersion relation $E(\mathbf{k})$ and DOS of FeGa₃ using GGA and DFT + *U* (with $\lambda = 3$ a.u.⁻¹) for the respective equilibrium volumes ($P = 0$ GPa), for an intermediate pressure ($P = 15$ GPa), and at high pressure ($P = 42$ GPa).

At $P = 0$ GPa, the GGA and DFT + *U* electronic structures present many similarities: in the whole energy range shown in Figs. 4(a) and 5(a), it is observed that the valence bands (vb) and conduction bands (cb) are built up from the hybridization of Fe *d* states (thick black lines) and Ga *s* and *p* states (thick red lines for Ga₁ and thick green lines for Ga₂). The valence band maximum (vbm) is located in the ZA direction, close to the A point, whereas the conduction band minimum (cbm) is located in the Γ Z direction. The difference between the calculated indirect band gaps is small, 0.34 eV for GGA and 0.42 eV for DFT + *U*. The character of the four top vb are dominated by Fe *d* states ($\sim 68\%$), and the contributions of Ga *s* and *p* states are evenly weighted ($\sim 16\%$ for each Ga type). The vbm eigenvalue character is mainly built up of Fe d_{xz} , d_{yz} , and a small contribution of $d_{x^2-y^2}$ orbitals, and there is a less significant contribution of Ga₁ *s* and p_z orbitals and Ga₂ p_x and p_y orbitals. Although the similarities of the electronic structure, especially in the cb, between GGA and DFT + *U* are remarkable, there are some important differences in $E(\mathbf{k})$, such as the obvious shift to lower energies of the top four vb (in the energy window between -0.17 and -0.82 eV) of the Fe *d* states due to the Hubbard *U* term. That shift is almost rigid, and the topology of the top two vb is basically not affected. However, there are remarkable differences for the second two vb in the ZA direction; for GGA these bands do not touch the next set of lower vb (which have more Ga *s* and *p* character), whereas for DFT + *U* these bands merge with those lower vb. As a result, the pseudogap observed in the GGA DOS at ~ -0.82 eV becomes less deep and wide with DFT + *U*. Another important difference in $E(\mathbf{k})$ is observed around the M point, where the bands located at ~ -1.1 eV for GGA rise to higher energy (~ -0.8 eV) when the Hubbard term is included.

The effect of external pressure on the electronic structure is already significant at the moderate value of 15 GPa [Figs. 4(b) and 5(b)]. First, the differences between GGA and DFT + *U* are almost nonexistent. The vbm is now located at the A point,

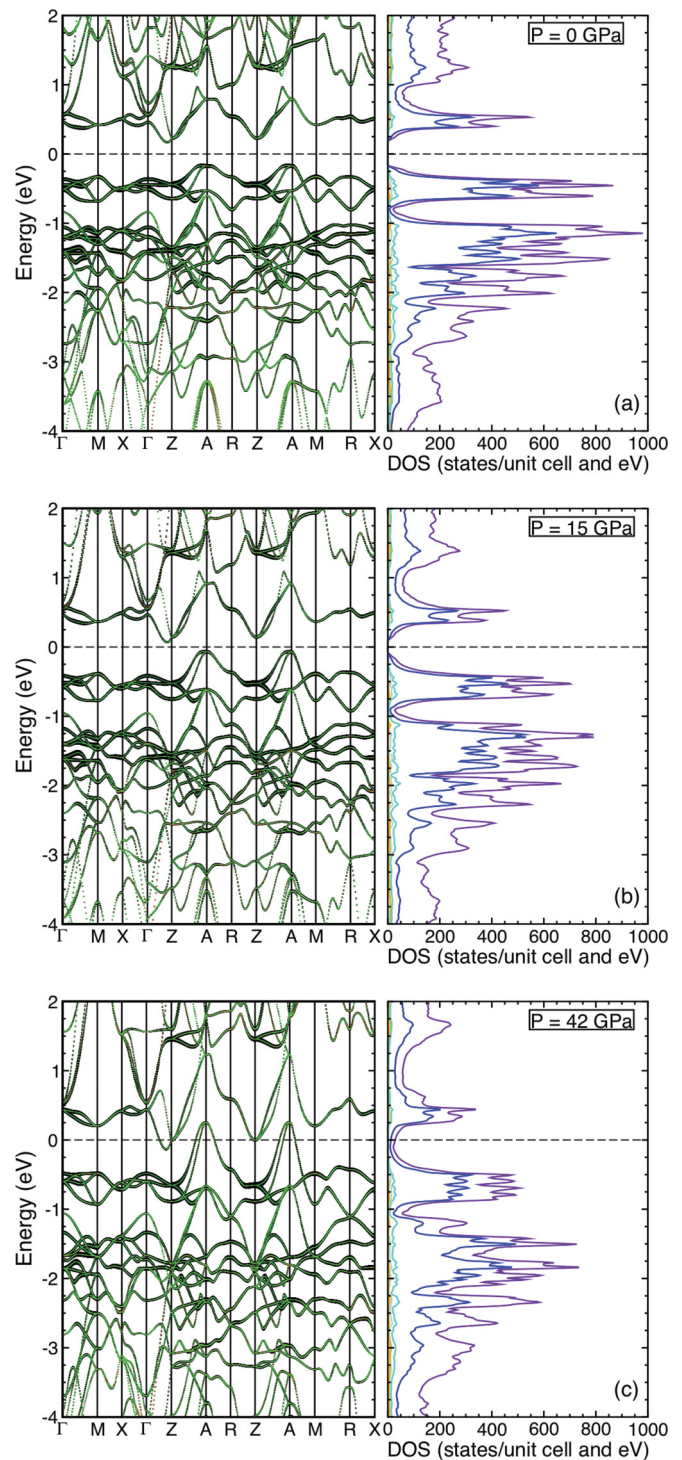


FIG. 4. (Color online) Calculated electronic structure with $\lambda \rightarrow \infty$ (GGA) for different pressures. For $E(\mathbf{k})$ the thick black lines correspond to Fe states, the thick red lines correspond to Ga₁ states, and the thick green lines correspond to Ga₂ states. The total DOS is denoted by a violet line, Fe *d* states are denoted by a blue line, Ga *s* states are denoted by an orange line, and Ga *p* states are denoted by a turquoise line. The energy is shifted to the Fermi level.

and the cbm is still located in the Γ Z direction, whereas the band gap becomes narrower. The character of the vbm has changed significantly, the Fe *d* states accounts for $\sim 58\%$, and

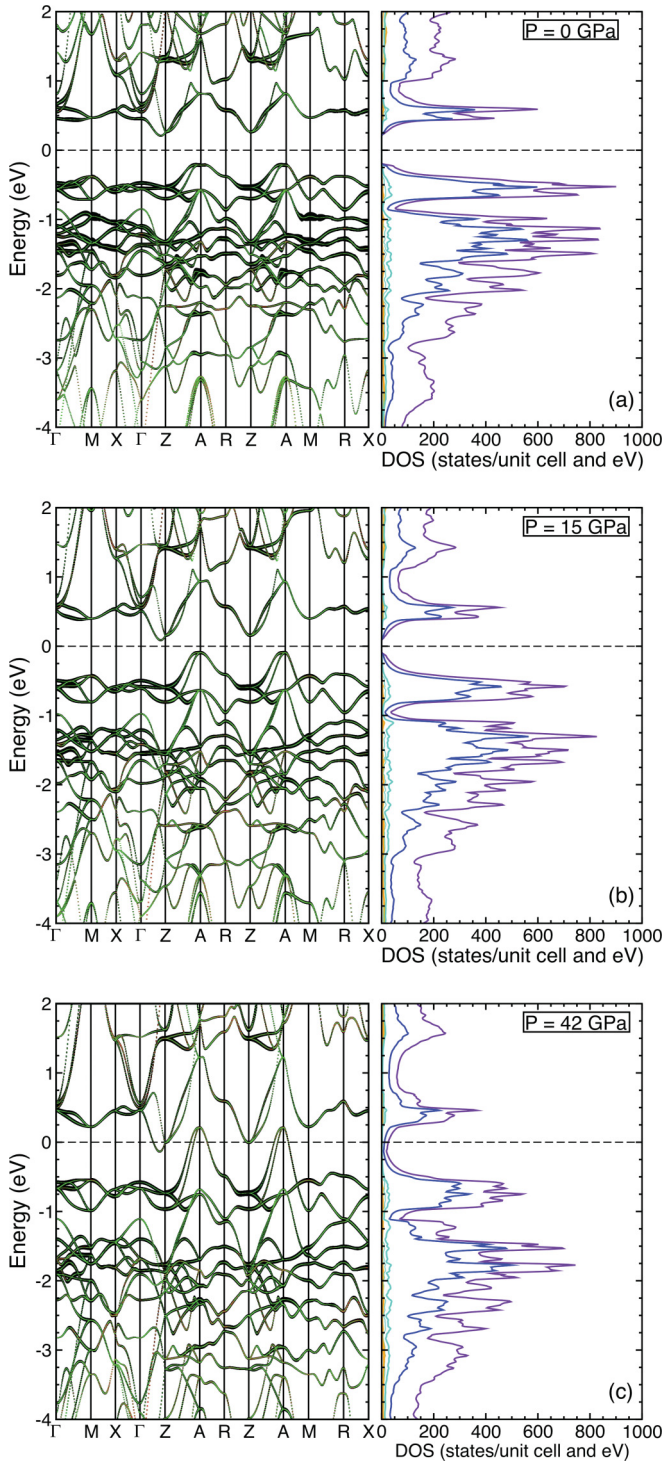


FIG. 5. (Color online) Calculated electronic structure with $\lambda = 3$ a.u.⁻¹ for different pressures. For $E(\mathbf{k})$ the thick black lines correspond to Fe states, the thick red lines correspond to Ga₁ states, and the thick green lines correspond to Ga₂ states. The total DOS is denoted by a blue line, Ga *s* states are denoted by an orange line, and Ga *p* states are denoted by a turquoise line. The energy is shifted to the Fermi level.

the contributions of Ga₁ and Ga₂ *s* and *p* states are $\sim 20\%$ and $\sim 22\%$, respectively. On the other hand, the gap at the Γ point has widened in comparison to the equilibrium volume. Also,

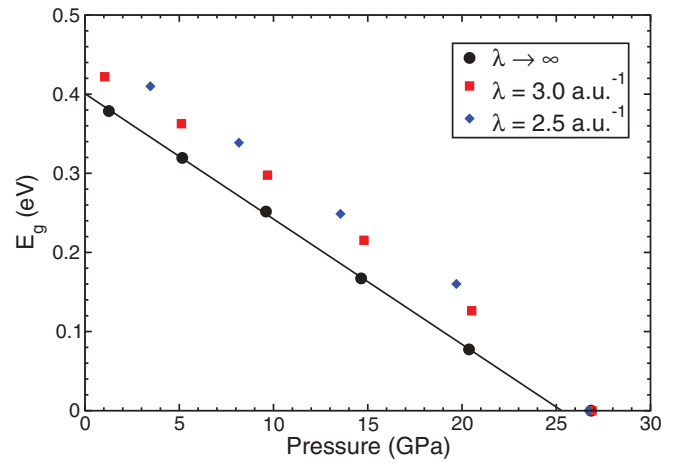


FIG. 6. (Color online) The calculated band gap as a function of pressure for different values of the Yukawa screening length. The black circles, red squares, and blue diamonds are the calculated band gaps for $\lambda \rightarrow \infty$, $\lambda = 3$, and $\lambda = 2.5$, respectively. The black line is a linear fit of the calculated GGA data.

the DOS is lower and wider. At this pressure the hopping term in the DFT + *U* Hamiltonian is completely dominant over the Hubbard *U* term, implying that the electronic correlation is weak and well described at the GGA level. The calculated electronic structure at the highest pressure reached in this study ($P = 42$ GPa) is shown in Figs. 4(c) and 5(c). As in the case of moderate pressure, the GGA and DFT + *U* electronic structures have no significant differences. One can observe that for this pressure a MIT has taken place, where the Fermi level now crosses the top two *vb* and the bottom two *cb* at lower pressures. These four conduction bands across the Fermi level show even more Ga *s* and *p* character ($\sim 54\%$), and the Fe *d*-state contribution decreases to $\sim 46\%$. Also, we can observe that the main peaks of the DOS are lower and wider.

The behavior of the band gap versus the applied pressure is shown in Fig. 6 for different values of the Yukawa screening length. The behavior of the band gap decreases linearly for GGA, with $\frac{dP}{d\Omega} = -0.016$, and the closure of the band gap occurs close to 25 GPa. For DFT + *U*, the behavior is almost linear for $\lambda = 3.0$ and deviates strongly from this behavior for $\lambda = 2.5$. Further, around $P = 27$ GPa the band gap is closed as well. The MIT is taking place in a pressure range where the change in the interionic Fe-Ga₂ distance becomes shorter than the distance between the Fe and Ga ions located on the same plane (Fe-Ga₁). This shortening of the Fe-Ga distances leads to a higher predominance of the Ga *s* and *p* states over the Fe *d* states around the Fermi level, which could be responsible for the present MIT.

IV. CONCLUSIONS

We have ruled out the presence of AF-SS magnetic order in FeGa₃, confirming that this compound is not magnetic. The electronic structure of this compound could be put into the regime of weakly correlated materials at its equilibrium

volume, and the effect of the external pressure leads it to a regime where GGA is sufficient to describe adequately its electronic structure, even at moderate pressures. We have also found that around a pressure of 25 GPa a metal-insulator transition takes place.

ACKNOWLEDGMENTS

This work was supported by FAPESP, CNPq, and CAPES (Brazil) and Vicerrectoría de Docencia-Universidad de Antioquia (Colombia). We thank Prof. M. A. Avila for fruitful discussions on this subject.

*jorge.osorio@fisica.udea.edu.co

- ¹D. Kasinathan, M. Wagner, K. Koepf, R. Cardoso-Gil, Y. Grin, and H. Rosner, *Phys. Rev. B* **85**, 035207 (2012).
- ²J. J. Pulikkotil, S. Auluck, P. K. Rout, and R. C. Budhani, *J. Phys. Condens. Matter* **24**, 096003 (2012).
- ³V. G. Storchak, J. H. Brewer, R. L. Lichti, R. Hu, and C. Petrovic, *J. Phys. Condens. Matter* **24**, 185601 (2012).
- ⁴R. Miao, G. Huang, C. Fan, Z. Bai, Y. Li, L. Wang, L. Chen, W. Song, and Q. Xu, *Solid State Commun.* **152**, 231 (2012).
- ⁵M. Arita, K. Shimada, Y. Utsumi, O. Morimoto, H. Sato, H. Namatame, M. Taniguchi, Y. Hadano, and T. Takabatake, *Phys. Rev. B* **83**, 245116 (2011).
- ⁶N. Haldolaarachchige, A. B. Karki, W. A. Phelan, Y. M. Xiong, R. Jin, J. Y. Chan, S. Stadler, and D. P. Young, *J. Appl. Phys.* **109**, 103712 (2011).
- ⁷E. Bittar, C. Capan, G. Seyfarth, P. Pagliuso, and Z. Fisk, *J. Phys. Conf. Ser.* **200**, 012014 (2010).
- ⁸Z. P. Yin and W. E. Pickett, *Phys. Rev. B* **82**, 155202 (2010).
- ⁹Y. Takagiwa, J. T. Okada, and K. Kimura, *J. Alloys Compd.* **507**, 364 (2010).
- ¹⁰Y. Hadano, S. Narazu, M. A. Avila, T. Onimaru, and T. Takabatake, *J. Phys. Soc. Jpn.* **78**, 013702 (2008).
- ¹¹N. Tsujii, H. Yamaoka, M. Matsunami, R. Eguchi, Y. Ishida, Y. Senba, H. Ohashi, S. Shin, T. Furubayashi, H. Abe *et al.*, *J. Phys. Soc. Jpn.* **77**, 024705 (2008).
- ¹²Y. Imai and A. Watanabe, *Intermetallics* **14**, 722 (2006).
- ¹³C. Lue, W. Lai, and Y. Kuo, *J. Alloys Compd.* **392**, 72 (2005).
- ¹⁴U. Haussermann, M. Bostrom, P. Viklund, O. Rapp, and T. Bjornangen, *J. Solid State Chem.* **165**, 94 (2002).
- ¹⁵P. Viklund, S. Lidin, P. Berastegui, and U. Haussermann, *J. Solid State Chem.* **165**, 100 (2002).
- ¹⁶F. Cricchio, O. Granas, and L. Nordstrom, *Phys. Rev. B* **81**, 140403 (2010).
- ¹⁷A. G. Petukhov, I. I. Mazin, L. Chioncel, and A. I. Lichtenstein, *Phys. Rev. B* **67**, 153106 (2003).
- ¹⁸F. Bultmark, F. Cricchio, O. Granas, and L. Nordstrom, *Phys. Rev. B* **80**, 035121 (2009).
- ¹⁹K. Dewhurst, S. Sharma, L. Nordström, F. Cricchio, F. Bultmark, and H. Gross, <http://elk.sourceforge.net>.
- ²⁰J. P. Perdew, A. Ruzsinszky, G. I. Csonka, O. A. Vydrov, G. E. Scuseria, L. A. Constantin, X. Zhou, and K. Burke, *Phys. Rev. Lett.* **100**, 136406 (2008).
- ²¹M. R. Norman, *Phys. Rev. B* **52**, 1421 (1995).
- ²²M. T. Czyzyk and G. A. Sawatzky, *Phys. Rev. B* **49**, 14211 (1994).
- ²³A. I. Liechtenstein, V. I. Anisimov, and J. Zaanen, *Phys. Rev. B* **52**, R5467 (1995).
- ²⁴V. I. Anisimov, I. V. Solovyev, M. A. Korotin, M. T. Czyzyk, and G. Sawatzky, *Phys. Rev. B* **48**, 16929 (1993).
- ²⁵A. Otero-de-la-Roza, D. Abbasi-Perez, and V. Luana, *Comput. Phys. Commun.* **182**, 2232 (2011).
- ²⁶A. Otero-de-la-Roza and V. Luana, *Comput. Phys. Commun.* **182**, 1708 (2011).